Supplementary Information: Controlling metal-organic framework crystallization via computer vision and robotic handling

Kai Xiang Chong[1], Qusai A. Alsabia[1], Zuyang Ye[1], Andrew McDaniel[1], Douglas Baumgardner[2], Dianne Xiao*[2], and Shijing Sun*[1]

[1]Department of Mechanical Engineering, University of Washington, 3900 E Stevens Way, NE, Seattle, WA 98195, USA.
[2]Department of Chemistry, University of Washington, Seattle, WA 98195-1700, USA.

*Corresponding authors: djxiao@uw.edu (Department of Chemistry) and shijing@uw.edu (Department of Mechanical Engineering), University of Washington, Seattle, WA 98195, United States

Contents

S1 Co_2(dobdc) synthesis dataset **S3**

S2 OT-2 liquid handling robot **S4**

S3 Data analysis **S5**

S4 Schematic of Human-Bok Choy Combined Workflow **S7**

S5 Computer vision algorithm: Bok Choy **S8**
S5.1 Scale bar detection S8
S5.2 Aspect ratio and area calculation S8
S5.3 Overlapping crystal identification and classification S8
S5.3.1 Activation criteria S8
S5.3.2 PCA for overlapping crystals S9
S5.3.3 Aspect ratio and area calculation and accuracy S9
S5.4 Additional figures and data S10

S6 Reproducibility and Image Selection for Crystallization Analysis **S12**

S7 Summary of Crystal Size and Shape Metrics **S13**

S1 Co_2(dobdc) synthesis dataset

The dataset CSV files store the batch number, synthesis ID, synthesis conditions, date imaged, microscope magnification, and synthesis procedures followed. The synthesis condition JSON contains the following synthesis parameters for each synthesis ID: temperature, reaction time, metal mass, ligand mass, and liquid volumes.

For batches and procedures, the corresponding JSON needs to be read to determine information such as steps followed for a procedure. Since synthesis conditions are commonly accessed, the information from the synthesis conditions JSON is also provided in the dataset CSV.

The synthesis conditions for Co_2(dobdc) were recorded and made publicly available in the UW Sun Lab GitHub repository

The repository contains the following key files:

- **batches.json** – Describes the total number of batches conducted during the project.
- **procedures.json** – Details the different synthesis parameters used for the synthesis of $_2$(dobdc).
- **synthesis_conditions.json** – Details the different synthesis parameters used for the synthesis of Co_2(dobdc).
- **mof_dataset.csv** – Contains structured data on the synthesis experiments, including:
  - Batch number
  - Synthesis ID
  - Magnification (X)
  - Image Path
  - Robot Pipette (Mara)
  - $Co(NO_3)_2$*$6H_2O$ (mg)
  - 2,5-Dihydroxyterephthalic Acid (mg)
  - Temperature (°C)
  - Reaction Time (hrs)
  - Solvent Volumes (Water, DMF, Ethanol in µL)
  - Date Taken

Table S1: Example synthesis conditions from `mof_dataset.csv`, showing part of the parameters used in the initial six conditions.

Batch Number	Synthesis ID	DI H_2O (μL)	DMF (μL)	EtOH (μL)	...
1	SolventVolumes-1I	3333.0	3333.0	3333.0	...
1	SolventVolumes-2I	5000.0	2500.0	2500.0	...
1	SolventVolumes-3I	4000.0	2000.0	4000.0	...
1	SolventVolumes-4I	2500.0	2500.0	5000.0	...
1	SolventVolumes-5I	6000.0	2000.0	2000.0	...
1	SolventVolumes-6I	2500.0	5000.0	2500.0	...

S2 OT-2 liquid handling robot

In this study, we utilized the OT-2 Opentrons Robot for automated high-throughput synthesis. Specifically, we used the OT-2 P1000 Single-Channel Pipette for our experiments. During the synthesis process, N, N-dimethylformamide (DMF), ethanol and water were placed in Mara for automated liquid handling. To evaluate the speed and accuracy of the OT-2, we conducted a benchmarking experiment using the P300 Single-Channel Pipette (300 µL capacity) as a reference.

To mimic the synthesis process, we set the aspiration and dispensing rate to their default value of 1. Additionally, both the blowout function (which expels residual liquid from the pipette tip) and the touch tip function were set to FALSE to ensure consistent liquid handling. The dispensing volume was set to 95 µL.

We measured the key performance metrics of the OT-2 robot: (a) Refill time (the time taken for the OT-2 to move from a 96-well plate to the reservoir, aspirate, and return to well plate): 7.56 seconds, (b) Cycle time (the time taken to dispense into a single well of 96-well plate): 2.03 seconds, and (c) Total operation time excluding axis-homing (Each well was filled with 95 µL of solution. Using a 300 µL pipette, the system aspirates 300 µL, dispenses into three wells, refills, and repeats): 498.3 seconds or 8 minutes and 18 seconds.

To evaluate the accuracy of the pipetting, the desired mass was set to 0.0950 g, while the actual mass of the dispensed solution was measured at 0.0949 g. Assuming the density of water is 1 g/cm3, the percentage error was calculated to be 0.105%, demonstrating the high precision and accuracy of the OT-2 pipetting system.

For comparison, manual pipetting of the same synthesis process took approximately 9 minutes and 21 seconds, which is comparable to the automated operation time of Mara. Therefore, while the overall speeds remain similar, the OT-2 robot significantly improved pipetting precision while simultaneously reducing manual labor and operator workload.

S3 Data analysis

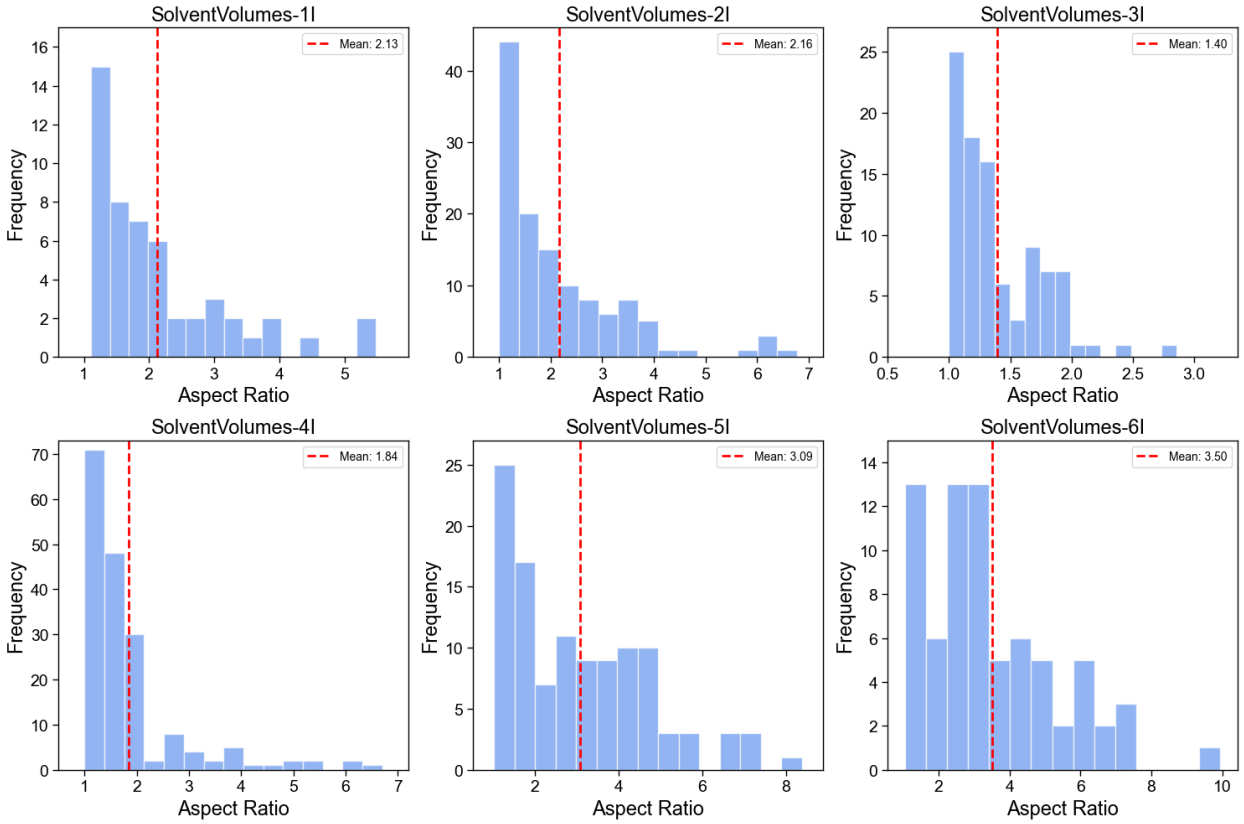

Figure S1: Histogram of the initial six synthesis conditions, displaying the mean values of the collected data.

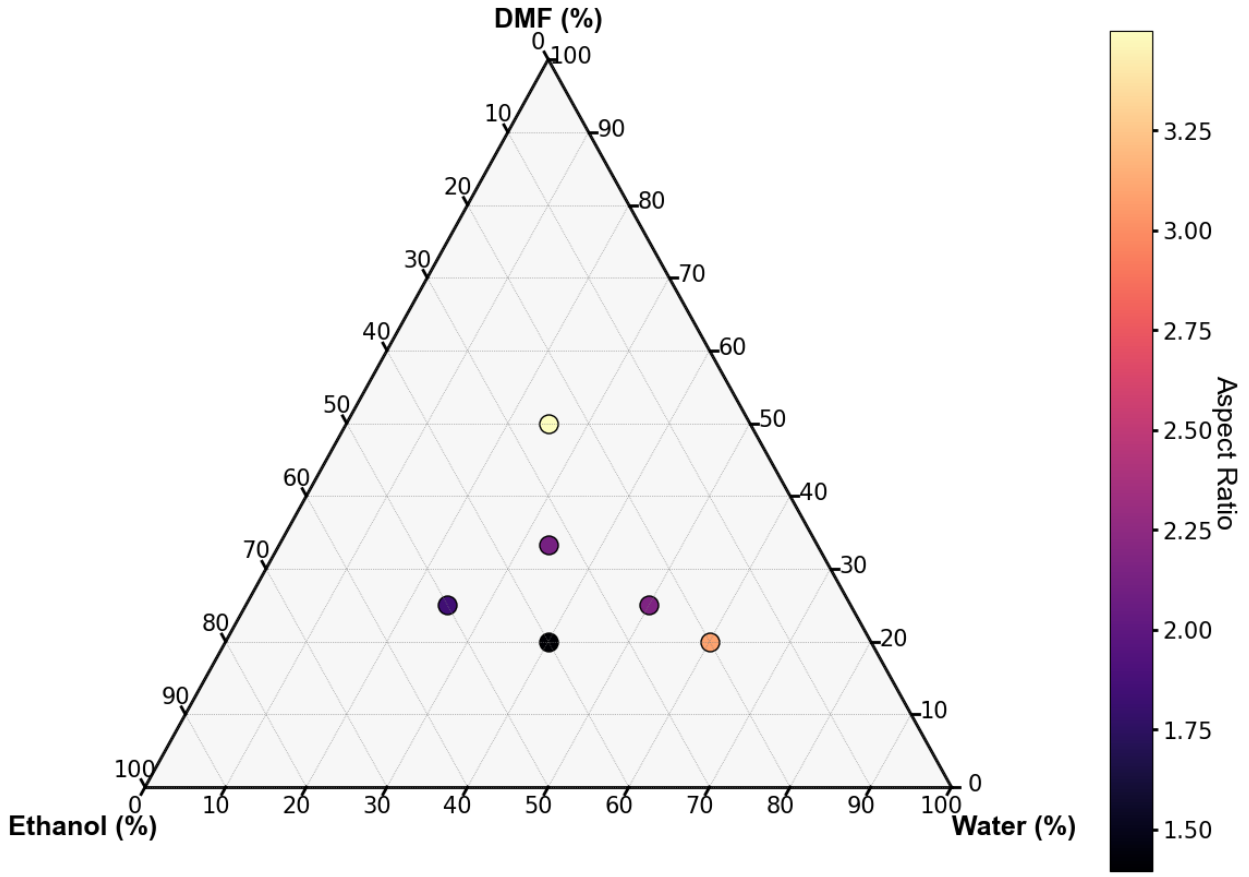

Figure S2: Ternary plot mapping the synthesis outcomes of Co_2(dobdc) under different solvent ratios, with color representing aspect ratios. The benchmarking synthesis conditions are highlighted.

S4 Schematic of Human-Bok Choy Combined Workflow

Images in the `README` file of the GitHub repository (`uwsunlab/Co-MOF`) present representative examples of microscopy data to highlight the capabilities and limitations of the Bok Choy algorithm. Human input is required at the initial stage to ensure reliable analysis. First, users confirm whether crystals are present in the image and image quality is satisfactory. Images classified as bad or those without visible crystals are deemed unsuitable for analysis by Bok Choy.

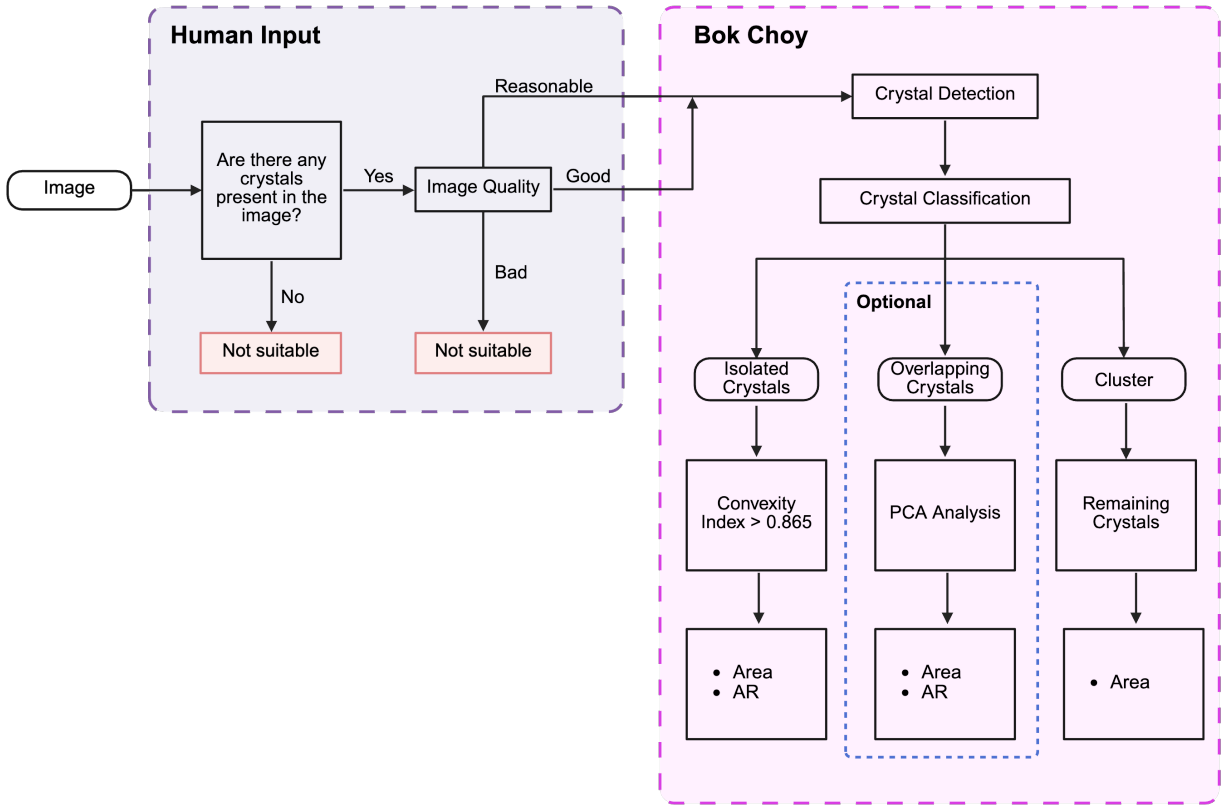

Figure S3: High-level workflow integrating human input and Bok Choy algorithm.

S5 Computer vision algorithm: Bok Choy

S5.1 Scale bar detection

Scale bar detection is handled by the ScaleBarDetector class and is composed of two main components. The first is an OCR (Optical Character Recognition) model from EasyOCR GitHub Repository that detects text, and the location of that text in the image. This text is then parsed using a regular expression to separate the numerical values of the text from the alphabetical parts. For example, if a slide has the text "200 μm", then the "200" would be separated from the "μm".

The second component of the ScaleBarDetector class finds the length in pixels of the longest contour in the image using OpenCV. This contour is assumed to be the contour corresponding to the scale bar. To further increase the likelihood that the correct contour is selected, a region of interest is defined surrounding the location of the text that was identified by the OCR model.

Dividing the numerical value of the text by the pixel length of the scale bar defines the units per pixel of the image; the actual units being defined by the alphabetical part of the OCR detection.

$$\text{Units per Pixel} = \frac{\text{Numerical Value from OCR}}{\text{Pixel Length of the Longest Contour}} \text{ (Unit)} \tag{S1}$$

S5.2 Aspect ratio and area calculation

For each filtered blue contours (isolated crystals and impurities), a minimum bounding box was plotted using the OpenCV library (`cv2.minAreaRect()`). The aspect ratio (AR) of the rectangle was then calculated using the following equation:

$$\text{AR} = \frac{\text{l}}{\text{w}} \tag{S2}$$

where AR represents the aspect ratio, l and w are the length and width of the rectangle.

The area of the isolated crystals and the clusters were calculated by first counting the total number of pixels within each contour. The real crystal area was then calculated by scaling the detected pixel area using the actual length obtained scale bar detection.

S5.3 Overlapping crystal identification and classification

S5.3.1 Activation criteria

To activate overlapping crystal detection, the `use_overlapping` flag must be set to `TRUE`, as shown in the CO-MOF/example_usage.ipynb `CO-MOF/example_usage.ipynb` file in the GitHub repository. When enabled, Bok Choy classifies contours into three categories: isolated crystals, overlapping crystals, and clusters. If images contain a large number of clusters,

it is recommended to disable overlapping crystals detection (`FALSE`) to improve classification accuracy and reduce misclassification.

S5.3.2 PCA for overlapping crystals

After isolated crystals were identified using convexity index thresholding (see Section 5.3), the remaining unclassified contours undergo a secondary analysis. The Probabilistic Hough Line Transform function (OpenCV) was applied to detect lines within each contour. Lines with similar orientations (within $\pm 10^{\circ}$, determined via trial and error across multiple images) were grouped.

To determine the bounding box of these grouped lines, **Principal Component Analysis (PCA)**, an unsupervised machine learning technique, was employed to extract the optimal dimensions (length and width) of each box. Since each group of lines has a different orientation, PCA transforms the image coordinate system into new principal axes. The first principal component corresponds to the longest directional spread (crystal length), while the second component represents the orthogonal direction (crystal width or thickness). PCA enables accurate alignment and shape measurement regardless of the crystals' rotation, eliminating the need to manipulate image orientation.

S5.3.3 Aspect ratio and area calculation and accuracy

Aspect ratios for overlapping crystal candidates were calculated as described in Section S5.2. These results were compared against those of isolated crystals. Contours were classified as overlapping crystals if their aspect ratio fell within the range of values observed for isolated crystals.

To compute the area, the image was binarized, and the total number of black pixels within the bounding box was counted. However, when compared to manual analysis using ImageJ, the calculated aspect ratio and area of overlapping crystals showed a percentage difference of 12.97% and 12.84%, respectively. Due to this reduced accuracy, overlapping crystals were excluded from downstream data analysis.

An example image in Figure S4 illustrates how the algorithm distinguishes between isolated crystals, overlapping crystals, and clusters. Contours not classified as isolated crystals or overlapping crystals were categorized as clusters.

S5.4 Additional figures and data

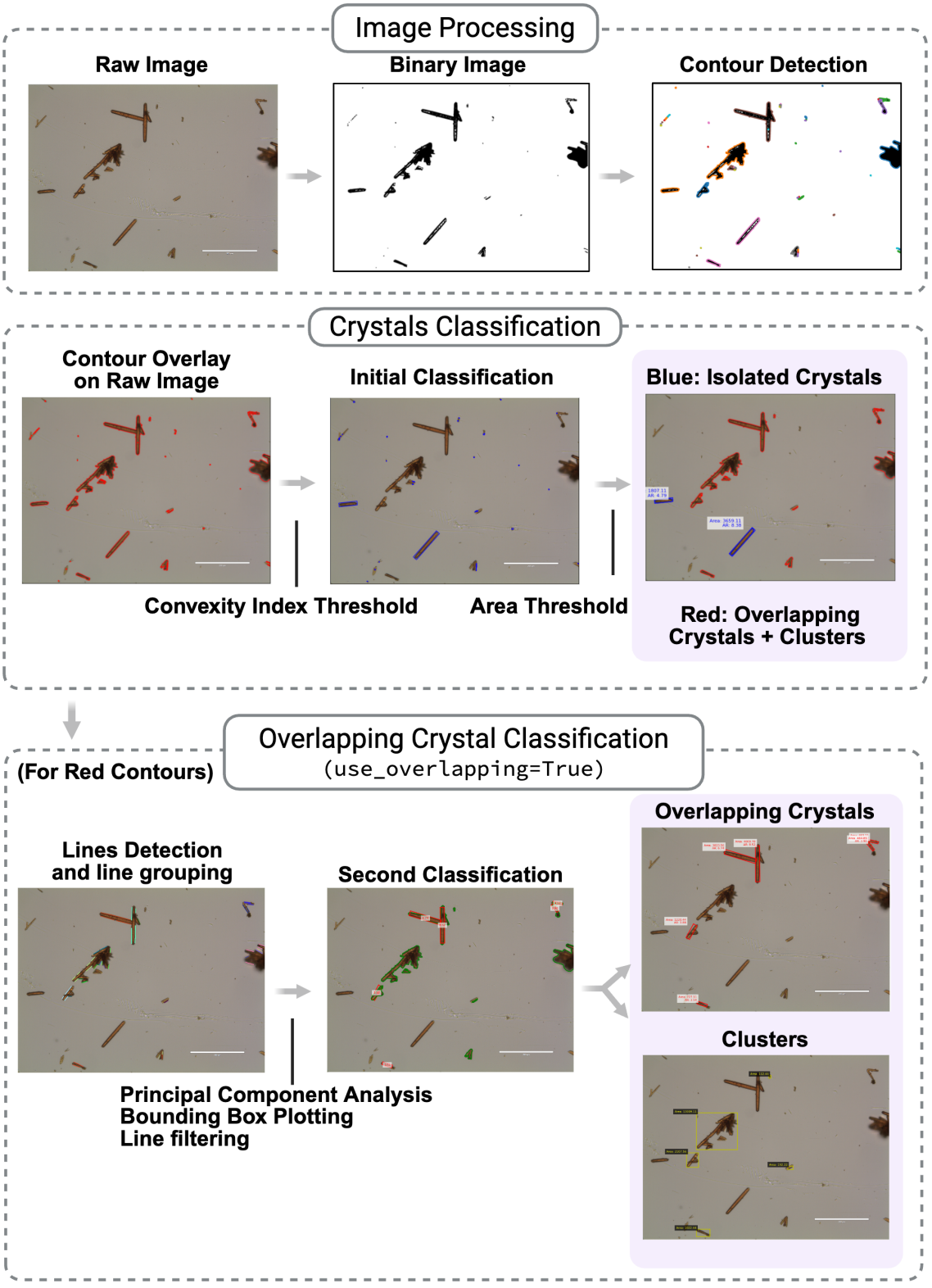

Figure S4: Extended workflow of the Bok Choy computer vision algorithm for crystal classification, including overlapping crystal detection. The process consists of three major stages: image processing, where raw images are converted into binary format for contour detection; crystal classification, which distinguishes isolated crystals (blue) from overlapping crystals and clusters; and overlapping crystal classification (refer to Section S5.3), where overlapping crystals (red) are further separated from clusters (yellow). Overlapping crystal detection is enabled by setting `use_overlapping=True`, which is disabled by default.

Table S2: Summary of crystals analyzed for the computation of Bok Choy's accuracy using Synthesis ID-5I. Each entry includes the crystal's corresponding image ID, aspect ratio, and area computed using both Bok Choy and ImageJ.

Crystal No	**Bok Choy**		**ImageJ**		**Differences**		**Image ID**
	AR	**Area (μm^2)**	**AR**	**Area (μm^2)**	**AR (%)**	**Area (%)**	
1	6.740	2846.33	7.1870	3300.44	6.22%	13.76%	EVOS_20X_020
2	5.480	2486.41	5.7040	2762.67	3.93%	10.00%	EVOS_20X_020
3	4.320	670.82	4.2630	768.89	1.34%	12.75%	EVOS_20X_020
4	3.850	847.03	4.1780	1138.67	7.85%	25.61%	EVOS_20X_023
5	3.100	1793.15	3.0770	1992.00	0.75%	9.98%	EVOS_20X_024
6	4.370	1706.94	4.3370	2035.11	0.76%	16.13%	EVOS_20X_024
7	4.440	2096.23	4.8570	2365.78	8.59%	11.39%	EVOS_20X_025
8	5.010	741.70	5.0070	908.44	0.06%	18.35%	EVOS_20X_025
9	4.720	707.93	4.7800	971.11	1.26%	27.10%	EVOS_20X_025
10	4.320	1659.39	4.3070	1920.44	0.30%	13.59%	EVOS_20X_025
11	3.950	1211.58	3.9400	1403.11	0.25%	13.65%	EVOS_20X_026
12	2.150	646.77	2.2350	696.44	3.80%	7.13%	EVOS_20X_026
13	5.170	1885.08	5.1200	2062.67	0.98%	8.61%	EVOS_20X_028
14	3.310	1654.79	3.5130	1928.89	5.78%	14.21%	EVOS_20X_028
15	4.750	2490.42	4.8210	2582.67	1.47%	3.57%	EVOS_20X_029
16	5.190	1892.26	5.1440	1972.44	0.89%	4.07%	EVOS_20X_029
17	5.730	3228.57	6.0990	3600.89	6.05%	10.34%	EVOS_20X_029
18	4.790	1811.14	4.6640	1941.78	2.70%	6.73%	EVOS_20X_031
19	8.380	3667.26	8.5100	4140.89	1.53%	11.44%	EVOS_20X_031
20	7.110	2163.03	7.4120	2363.56	4.07%	8.48%	EVOS_20X_032

Average Differences (%): 2.93% (AR), 12.35% (Area)

S6 Reproducibility and Image Selection for Crystallization Analysis

To assess the reproducibility of crystallization outcomes across different synthesis conditions, we conducted 23 unique Co-MOF-74 syntheses, each repeated three times (Batches 5, 6, and 7). Batches 5 and 6 were prepared using the Opentrons OT-2 liquid handling robot to ensure precise and consistent pipetting, while Batch 7 was synthesized manually to evaluate the reproducibility across automation methods.

Figure S5 presents the ternary diagrams comparing the crystallization outcomes across Batch 5 and 6, which shared identical synthesis condition IDs. These plots show high consistency across batches, supporting the reproducibility of our observations. However, inconsistencies were observed for Conditions 12II, 14II, and 23II (see ESI section S1 for full synthesis parameters), where clusters were detected for Batch 5, while Batch 6 showed isolated crystals. These differences might arise from variability in sample dilution during transfer to the imaging plate, which affected the spatial dispersion of crystals. For Condition 20II, no crystallization was observed in Batch 5, but isolated crystals appeared in Batch 6. This discrepancy may be attributed to the localized distribution of crystals within the well, as imaging was performed from selected fields of views, or due to variabilities incurred during manual pipetting into the 96-well plate prior to imaging.

To further validate this reproducibility, seven synthesis conditions were independently repeated in Batch 7 to compare results from automated and manual synthesis specifically. The crystallization results from Batch 7 were consistent with those of Batch 6, as shown in Figure S5b. Refer to the images in the co-mof dataset for access to the complete dataset from Batch 7.

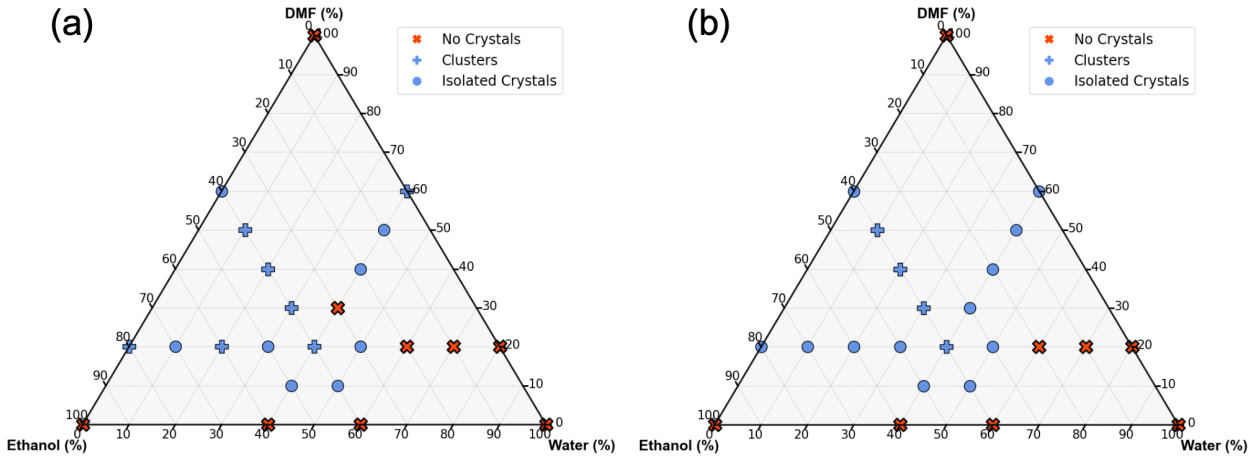

Figure S5: Ternary plot comparing crystallization outcomes for Batch 5 (a) and Batch 6 (b) under identical synthesis conditions.

As described in the "Human-Bok Choy Combined Workflow" section (Figure S3), human input plays a critical role in selecting high-quality microscopy images for analysis. Each image was assessed based on (1) the presence or absence of crystals and (2) its overall quality, which was categorized as good, reasonable, or bad.

This human validation step ensured only the most analyzable images were selected. When multiple images existed for the same synthesis condition across different batches, the highest-quality image was prioritized. For example:

- If Batch 5 showed clustering but Batch 6 produced isolated crystals under the same conditions, the image from Batch 6 was selected for aspect ratio and crystal area determination.
- If Batch 5 showed no crystallization but Batch 6 and 7 did, the ternary diagram in Figure 5 was updated to reflect the average results across Batch 6 and 7.

If no microscopic images were available from Batch 5 and Batch 6 for certain conditions, it was because no crystallization occurred in those specific experiments.

It is important to note that the observed separation between isolated and clustered crystals is partially influenced by the dilution step prior to imaging. Greater dilution tends to disperse crystals more effectively, reducing clustering seen in the images. The crystallization database and ternary diagram reflect actual experimental observations, captured from specific fields of view across the well plates.

S7 Summary of Crystal Size and Shape Metrics

Table S3: Summary of synthesis conditions and their corresponding Bok Choy image analysis results. Tables highlighted in red indicate conditions where no crystallization occurred, while blue highlights indicate the presence of significant crystal clustering.

Synthesis Condition	***Aspect Ratio***	***Area***
SolventVolumes-1I	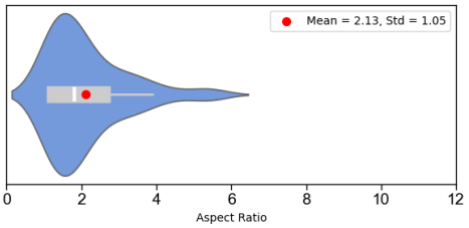	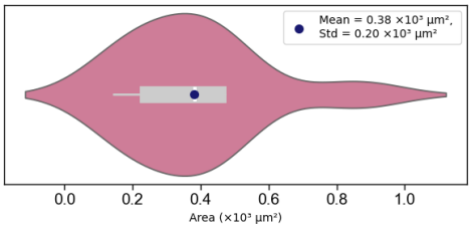
SolventVolumes-2I	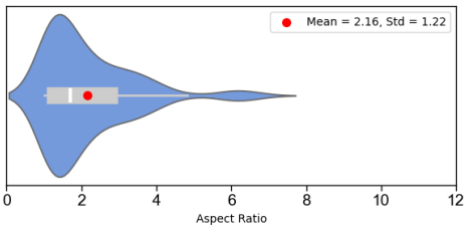	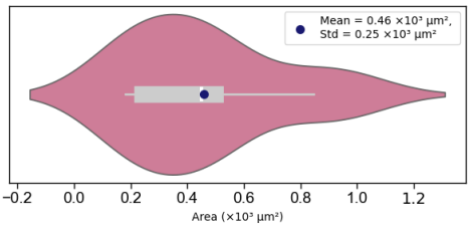
SolventVolumes-3I	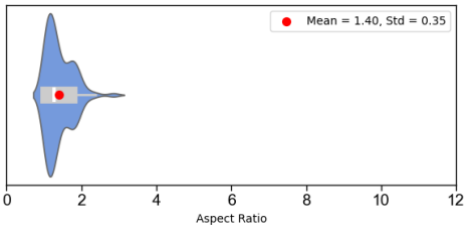	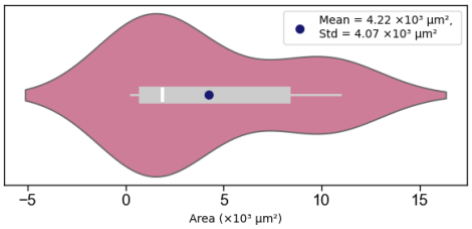
SolventVolumes-4I	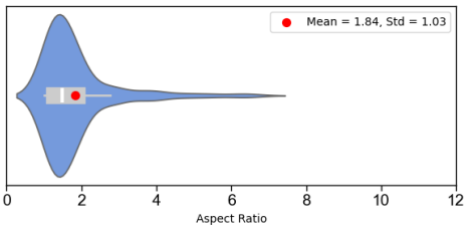	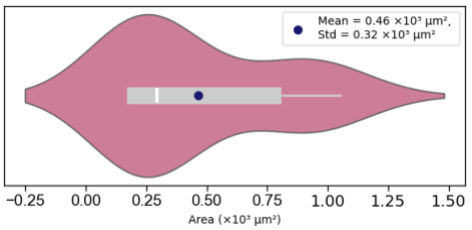
SolventVolumes-5I	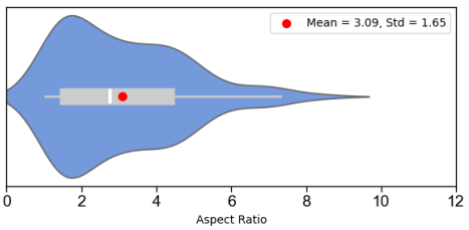	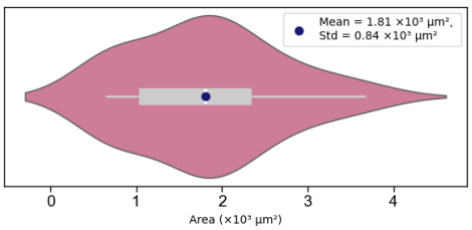
SolventVolumes-6I	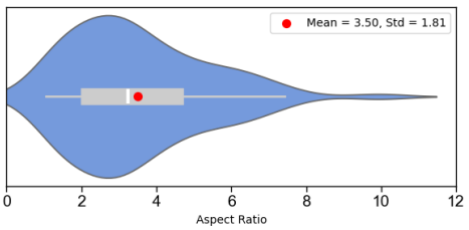	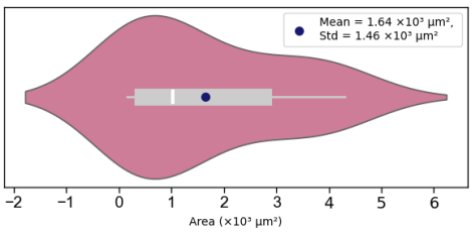
Time1		

Time2

Time3

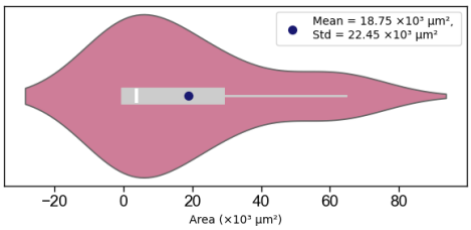

Time4

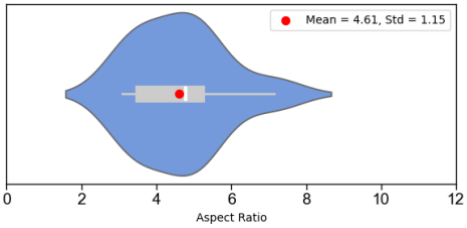

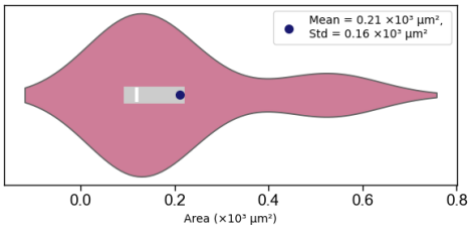

Time5

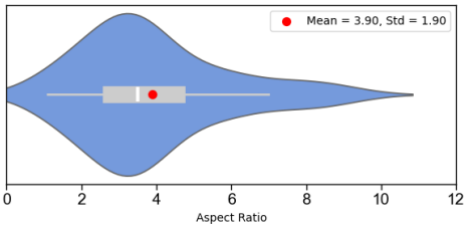

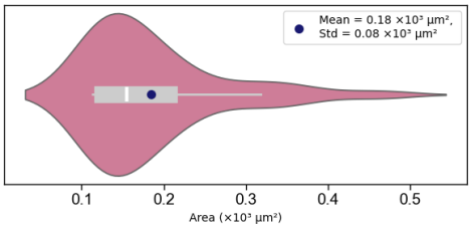

Time6

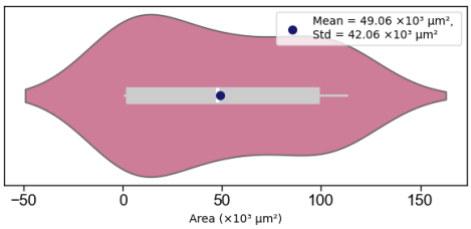

Temperature1

Temperature2

Temperature4

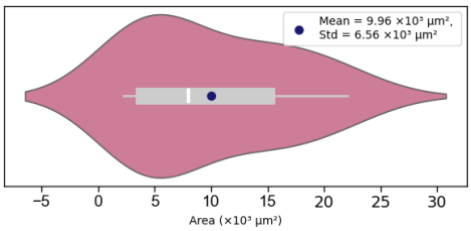

Temperature5

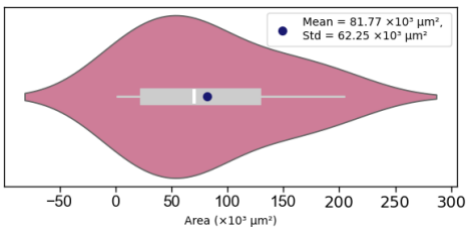

Modulator-Linker1		
Modulator-Linker2		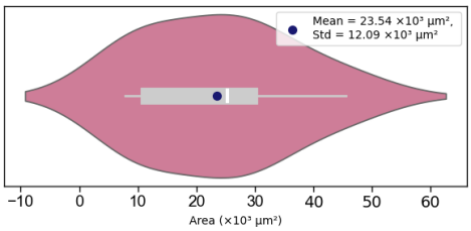
Modulator-Linker3		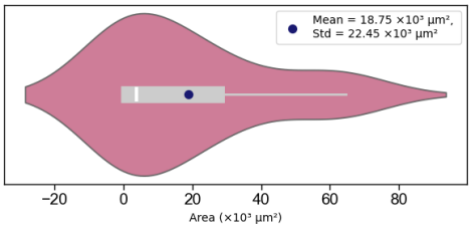
Modulator-Linker4		
Modulator-Linker5		
Modulator-Linker6		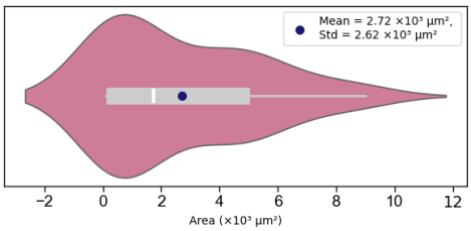
Modulator-Linker7	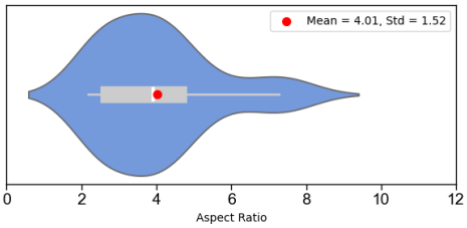	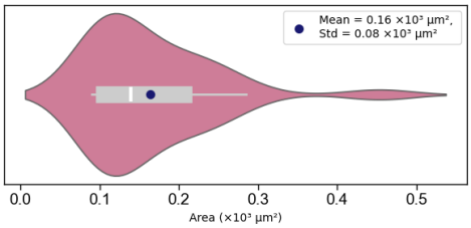
Modulator-Linker8	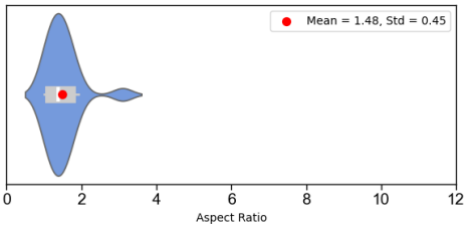	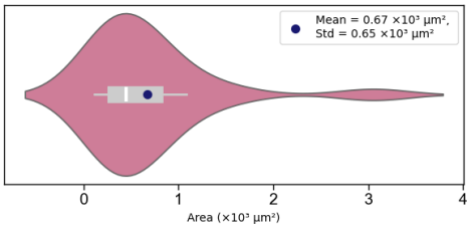
Modulator-Linker9		
Modulator-Linker10		

Modulator-Linker11		
SolventVolumes-1II		
SolventVolumes-2II	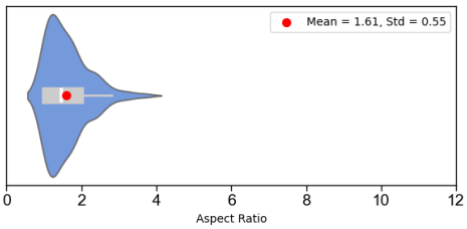	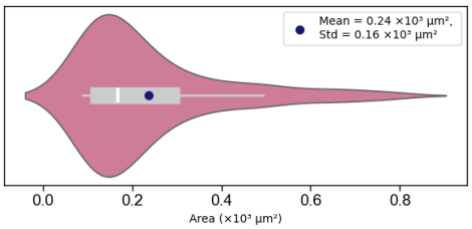
SolventVolumes-3II		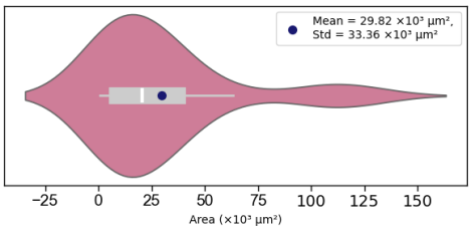
SolventVolumes-4II		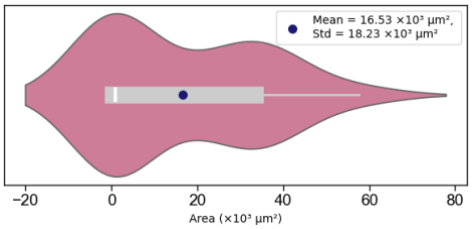
SolventVolumes-5II		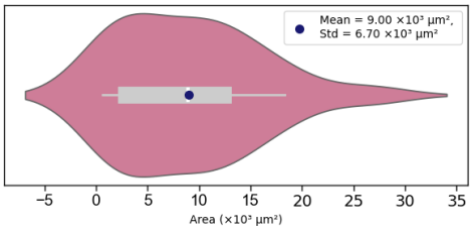
SolventVolumes-6II	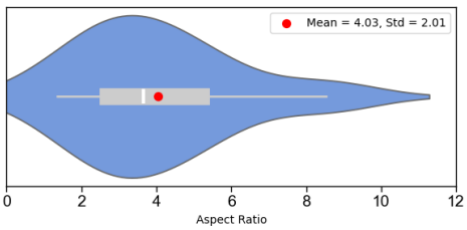	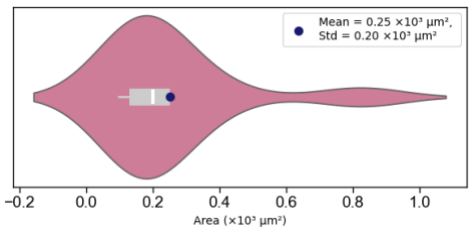
SolventVolumes-7II		
SolventVolumes-8II		

SolventVolumes -9II		
SolventVolumes -10II	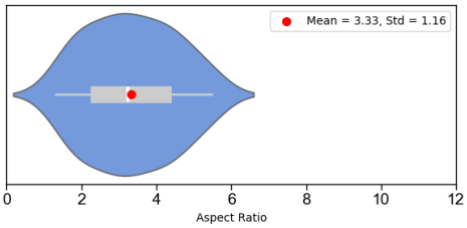	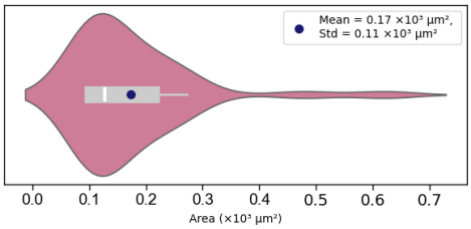
SolventVolumes -11II	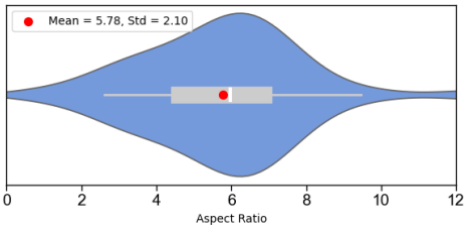	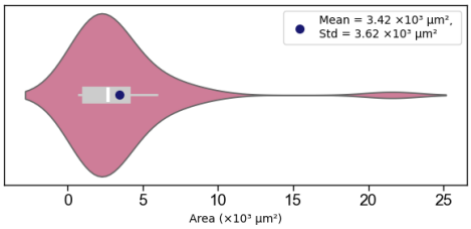
SolventVolumes -12II	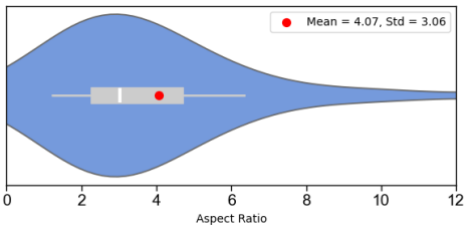	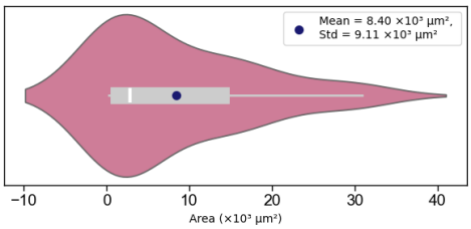
SolventVolumes -13II	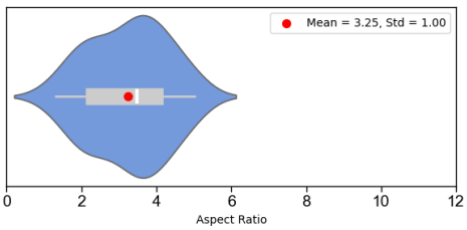	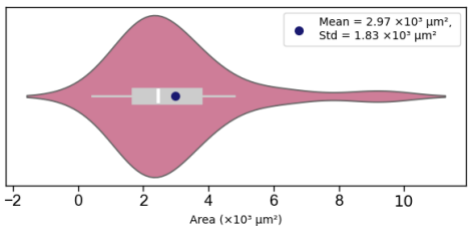
SolventVolumes -14II	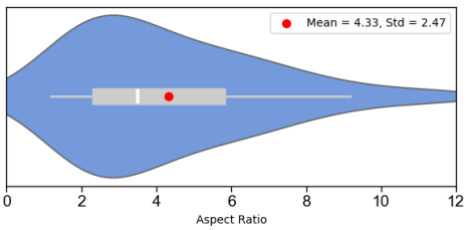	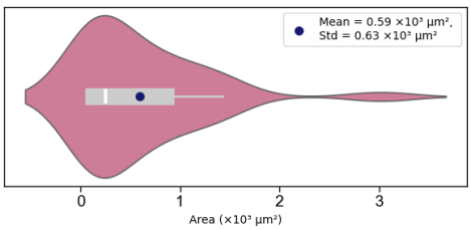
SolventVolumes -15II		
SolventVolumes -16II		
SolventVolumes -17II		

SolventVolumes -18II

SolventVolumes -19II

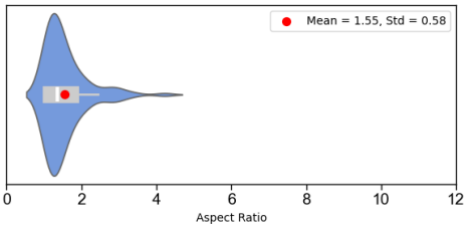

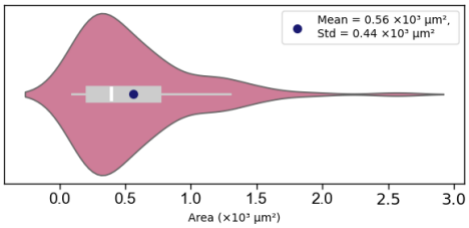

SolventVolumes -20II

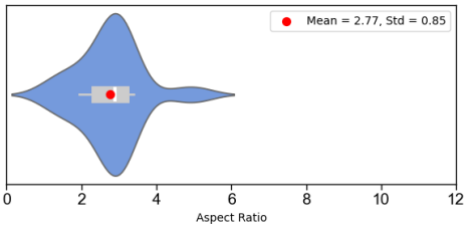

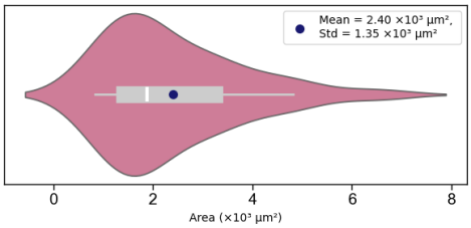

SolventVolumes -21II

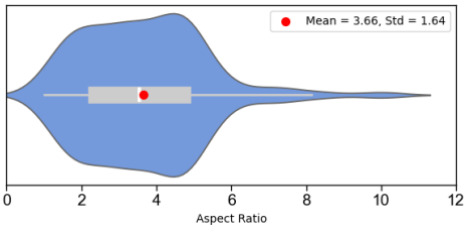

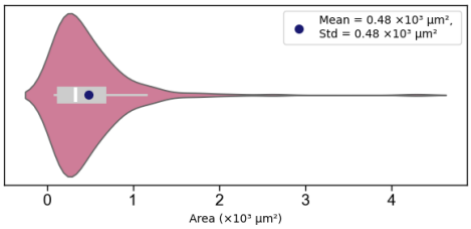

SolventVolumes -22II

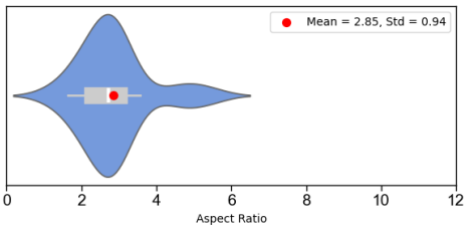

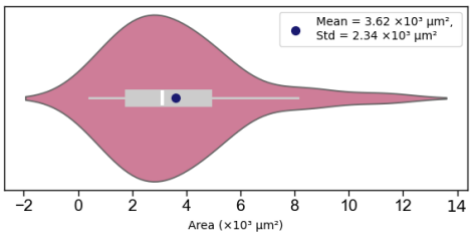

SolventVolumes -23II